State of the Art in Monitoring Rotating Machinery – Part 2

Robert B. Randall, The University of New South Wales, Sydney, Australia

In the last thirty years there have been many developments in the use of vibration measurement and analysis for monitoring the condition of rotating machinery while in operation. These have been in all three areas of interest, namely fault detection, diagnosis and prognosis. Of these areas, diagnosis and prognosis still require an expert to determine what analyses to perform and to interpret the results. Currently much effort is being put into automating fault diagnosis and prognosis. Major economic benefits come from being able to predict with reasonable certainty how much longer a machine can safely operate (often a matter of several months from when incipient faults are first detected). This article discusses the different requirements for detecting and diagnosing faults, outlining a robust procedure for the former, and then goes on to discuss a large number of signal processing techniques that have been proposed for diagnosing both the type and severity of the faults once detected. Change in the severity can of course be used for prognostic purposes. Most procedures are illustrated using actual signals from case histories. Part 1 of this article appeared in the March 2004 issue of S&V.

AR Models. AR or 'autoregressive' models are more efficient where there are sharp spectral peaks, and thus the required transfer function has poles. This is the case with IIR (infinite impulse response) filters where outputs are generated recursively from the previous outputs and the current input.

The relationship between input and output signals can be expressed as:

$$y_i = -\sum_{k=1}^{N} a_k y_{i-k} + x_i \tag{11}$$

which after Z-transformation gives:

$$Y(z)A(z) = X(z) \tag{12}$$

from which comes the transfer function:

$$\frac{1}{A(z)} = \frac{1}{\sum_{k=0}^{N} a_k z^{-k}} = \frac{1}{\prod_{k=1}^{N} \left(1 - z^{-1} p_k\right)} \tag{13}$$

which has no zeros and is an all-pole model.

There are a number of techniques that result in such an AR model, one of which is the "maximum entropy" method. In this, the coefficients are found by maximizing the entropy (disorder) of the signal, while ensuring that the autocorrelation function is determined by the signal within the window. This really means that the signal outside the window will be most similar to the signal within the window because of the elimination of any biasing effect. Other AR techniques include "linear prediction" and statistical 'autoregression' from which AR modeling takes its name.

Figure 11 shows the results of applying maximum entropy analysis to a very short record of envelope signal from a bearing with an inner race fault.[12] The record length comprised only 1.29 revolutions of the shaft speed which determined the spacing of modulation sidebands in the envelope spectrum. The maximum entropy spectrum of Figure 10d appears to give very good resolution of the sidebands, but Figure 10c shows that Fourier analysis can give almost as much information pro-

---

Based on a paper presented at ISMA 2002, the International Conference on Noise and Vibration Engineering, Leuven, Belgium, September, 2002.

vided a sufficient degree of spectrum interpolation is used. The spectrum interpolation was achieved by padding the data record with zeros to seven times its original length. Note that the maximum entropy spectrum had to be represented on a logarithmic amplitude scale because of the much wider range of amplitude values than for the Fourier analysis cases.

AR modeling has recently been applied to the detection of local faults on gears.[13] A model is developed for the signal from an undamaged section of a gear using linear prediction, and when a damaged section of the gear enters the mesh, the actual value of the signal departs dramatically from the linearly predicted value and the 'error' gives a measure of the local change. Fault indication using AR modeling gives better results than the 'residual' method used earlier.[13] The latter is based on removing the normal gearmesh signal obtained by synchronous averaging.

AR and MA models can be combined to give so-called ARMA models with both poles and zeros, but these are used more for system modeling than spectrum analysis.

Separation of Periodic and Random Signals. Machine signals are often very complex with mixtures of periodic and random signals, and mixtures of signals with different periodicity. It can be advantageous to separate the different components from each other.

Synchronous Averaging. The most widely used technique for separating different signals is time synchronous averaging, which is useful to extract that part of a signal having the same period as a trigger signal (e.g. a once-per-rev tacho signal from a shaft in a rotating machine). In practice it is done by averaging together a series of signal segments each corresponding to one period of the synchronizing signal. Thus:

$$y_a(t) = 1/N \sum_{n=0}^{N-1} y(t + nT) \tag{14}$$

This can be modelled as the convolution of $y(t)$ with a train of N delta functions displaced by integer multiples of the periodic time T, which corresponds in the frequency domain to a multiplication by the Fourier transform of this signal. This is given by the expression:[14]

$$C(f) = 1/N \sin(N\pi Tf)/\sin(\pi Tf) \tag{15}$$

The filter characteristic corresponding to this expression is shown in Figure 12 for the case where $N = 8$, a comb filter selecting the harmonics of the periodic frequency. The greater the value of N the more selective the filter, and the greater the rejection of nonharmonic components. The noise bandwidth of the filter is $1/N$, meaning that the improvement in signal/noise ratio is $10 \log_{10} N$ dB for additive random noise. For masking by discrete frequency signals, it should be noted that the characteristic has zeros that move with the number of averages, so it is often possible to choose a number of averages that completely eliminates a particular masking frequency. The above characteristic is for an infinitely long time signal $y(t)$. For the practical situation of a finite length of signal with finite sampling frequency, it is possible to calculate an optimum number of averages to completely remove a discrete masking signal, in particular when the frequency is related by a rational fraction to the synchronous frequency.[14] This is always the case for different shafts in gearboxes.

For good results the synchronizing signals should correspond exactly with samples of the signal to be averaged. One sample spacing corresponds to 360° of phase of the sampling
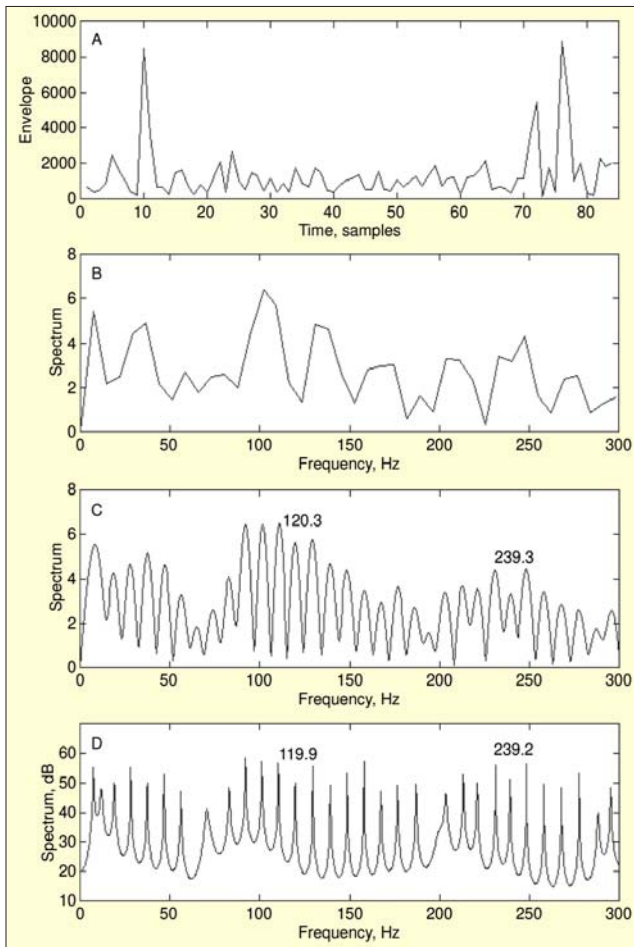
Figure 11. Envelope spectra of a very short length of signal (1.29 periods of shaft rotation). A – Envelope signal, B – Direct FFT spectrum, C – Interpolated FFT spectrum, D – Maximum entropy spectrum.
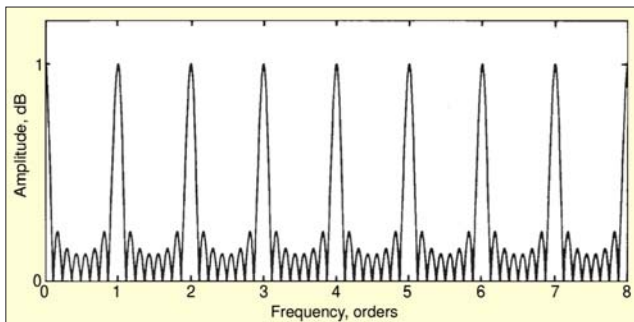

Figure 12. Filter characteristic for 8 averages.[14]

frequency, and thus to 144° of phase at 40%, a typical maximum signal frequency. Moreover, even a 0.1% speed fluctuation would cause a jitter of the same order of the last sample in a (typical) 1k record with respect to the first, and thus an even greater loss of information at the end of the record after averaging.

Sampling the signal using a sampling frequency derived from the synchronizing (tacho) signal as described below solves both of these problems and is always to be recommended. Figure 13 shows the results of using synchronous averaging on speed corrected data from a gearbox in a variable speed mining shovel (see Figure 14). The order tracked data was arranged to have an integer number of samples per period of the low speed gear, which allowed determination of the harmonics of this gear speed by synchronous averaging. The spectrum of this signal is shown in Figure 14a. After a periodic repetition of this signal was subtracted from the overall tracked signal, the data were resampled to have an integer number of samples per period of the high speed gear, after which its harmonics could be
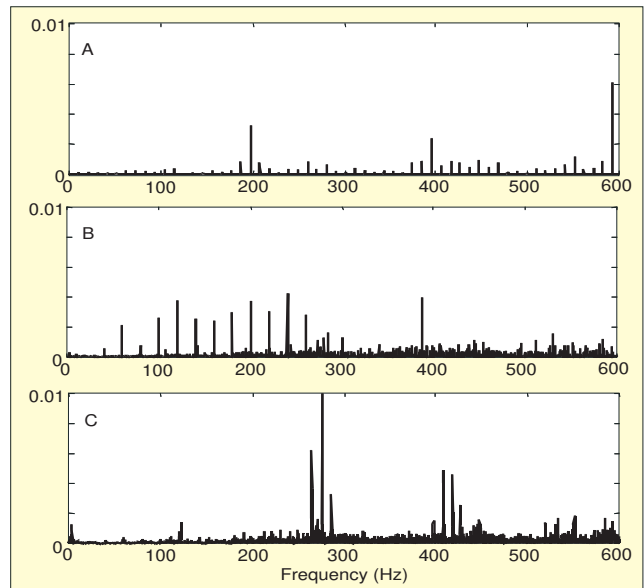

Figure 13. Application of synchronous averaging to a mixture of gear and bearing signals. A – spectrum from low speed gear, B – spectrum from high speed gear, C – spectrum of residual signal (bearing fault).
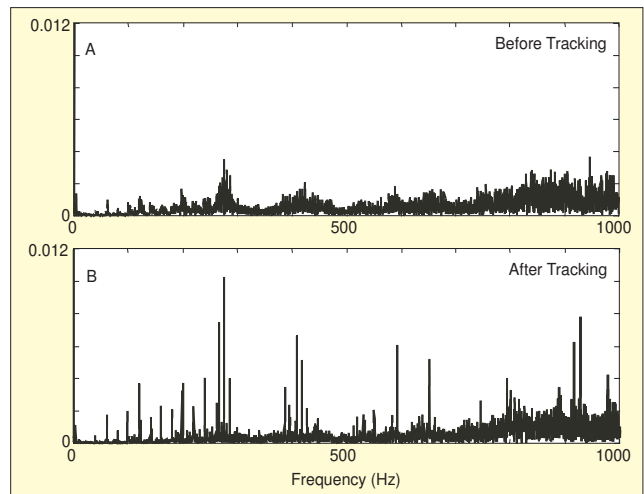

Figure 14. Use of tracking to avoid smearing of shaft speed related components.

determined in the same way (Figure 13b). Finally, after subtraction of this periodic signal from the data, the remaining signal was dominated by the effects of an inner race bearing fault (Figure 13c).

Order Tracking. In analyzing rotating machine vibrations, an x-axis based on harmonics or 'orders' of shaft speed is often desirable. This can avoid smearing due to speed fluctuations or show how the strength of the various harmonics changes over a greater speed range, such as when they pass through various resonances. For example, if a constant amplitude signal that is synchronous with the rotation of a shaft is sampled a fixed number of times per revolution, the digital samples are indistinguishable from those of a sinusoid and thus give a line spectrum. On the other hand, if normal temporal sampling is used, the spectrum spreads over a range corresponding to the variation in shaft speed. Thus, for order analysis it is necessary to generate a sampling signal from a tacho signal synchronous with shaft speed. It is sometimes possible to use a shaft encoder mounted on the shaft in question to provide a sampling signal, but more often the latter has to be generated electronically. Formerly, this was done using a phase-locked loop to track the tacho signal and then generate a specified number of sampling pulses per period of the tracked frequency. However, an analog phase-locked loop has a finite response time and cannot necessarily keep up with the random
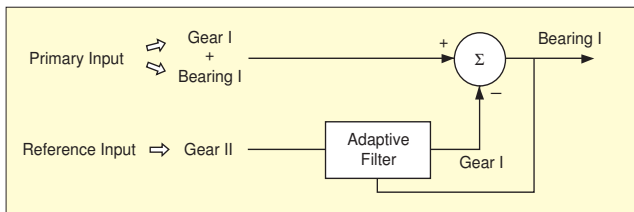
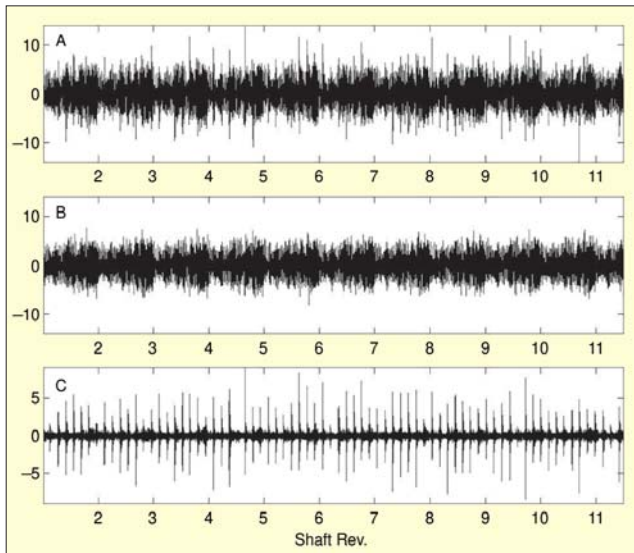Figure 15. ANC applied to separation of bearing and gear signals.

Figure 16. Separation of (additive) gear and bearing signals using DRS. A – combined signal, B – deterministic part (gear signal), C – stochastic part (bearing signal).
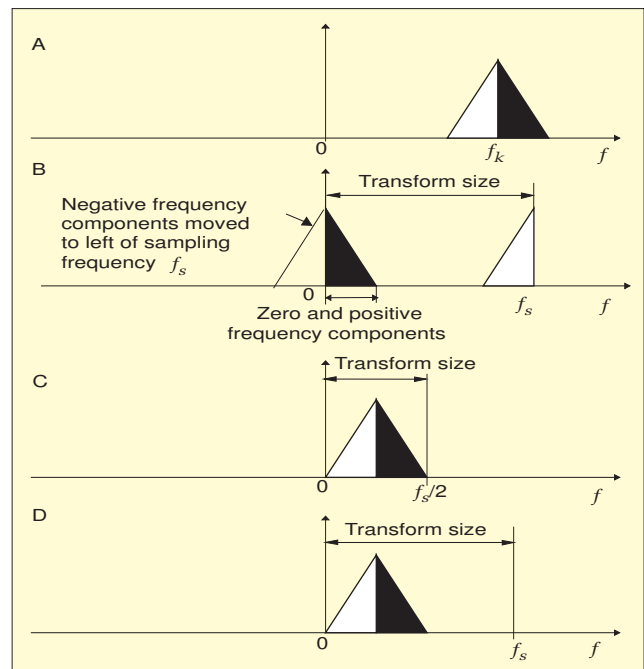

Figure 17. Block shift procedure for selecting frequency band for demodulation. A – original spectrum of one-sided bandpass section, B – Frequency shift by f_k (center of passband), C – frequency shift by amount corresponding to lower passband limit (half size transform – not recommended), D – frequency shift by amount corresponding to lower passband limit (full size transform).

speed fluctuations that occur with an internal combustion engine from cycle to cycle. The best method is to digitally resample each record based on the corresponding period of the tacho signal. This can be done in a number of ways, based on digital interpolation.[15]

Quite apart from errors introduced by the interpolation, when resampling at a lower frequency (for example as a machine speed reduces), it is necessary to ensure that the signal is adequately lowpass filtered to prevent aliasing. Digital filtering can be useful here as the cutoff frequency varies directly with the sampling frequency, but the initial analog lowpass filtration must be such that aliasing components do not enter the measurement range. Digital oversampling can solve this problem, as the sampling frequency can be reduced by a large factor before overlap occurs.

Figure 14 illustrates the use of tracking to avoid smearing in the spectrum of the vibration signal from a gearbox. The discrete frequency components in the spectrum after tracking come mainly from gear-related components that were removed using synchronous averaging as shown in Figure 13.

Adaptive Noise Cancellation. Adaptive noise cancellation (ANC) is a method for separating two signal components (in a primary signal) where there is access to another (reference) signal containing only one of the two components. The reference signal does not have to be identical to the related component in the primary signal, just coherent with it so that they are related by a linear transfer function.[16] Figure 15 illustrates the basic principle applied to a situation where the primary signal contains both gear and bearing (fault) components. These could be measurements on a faulty bearing where the reference signal contains only a gear signal, for example measured on a more remote bearing. The adaptive filter adjusts its coefficients so as to minimize the power of the error signal, the difference between the primary and filtered reference inputs. When the two components are statistically independent, this separates them and the error signal becomes the bearing signal.

Another development of this, self adaptive noise cancellation (SANC), uses the difference in statistical properties of the two components (as discussed in the section on bearing faults) to separate them. The deterministic gear signal has a much longer correlation length than the stochastic bearing signal, hence the reference signal can be a delayed version of the primary mixture, so that only the deterministic gear signals are coherent.[8]

In separating gear and bearing signals, most often the signals are stationary (order tracking may have to be used to ensure this), and therefore there is no need to continually adapt the filter. In such situations a new method called DRS (discrete/random separation) has recently been proposed that achieves virtually the same result much more efficiently.[17] First a transfer function is found between the current signal and a delayed version, which results in a comb filter corresponding to the discrete frequency components (coherent even with a delay). The amplitude of this transfer function is then used as a (zero phase shift) filter to transmit the deterministic part and reject the random part. Both the filter generation and the subsequent filtering are done using FFT techniques, making the whole procedure much more efficient than the SANC approach. The difference compared with synchronous averaging is that the discrete frequency components are not required to have harmonic relationships.

Figure 16 shows an application involving separation of a discrete frequency gear signal from an inner race bearing fault signal, which despite its periodic appearance is actually random. After separation, envelope analysis gives a clear diagnosis of the bearing fault.

Demodulation. Modulation occurs when an otherwise sinusoidal signal, a so-called carrier signal, has its amplitude or frequency made to vary with time. The first case is amplitude modulation and the second can be considered frequency or phase modulation. Phase modulation is the deviation in phase (angular displacement) from the linearly increasing phase of the carrier, while frequency modulation is the difference in instantaneous frequency (angular velocity) from the constant carrier frequency. Thus, frequency modulation is the derivative of phase modulation. A direct mechanical example of phase/frequency modulation is shaft torsional vibration. When expressed in terms of shaft angle, it is a phase modulation. When expressed in terms of shaft speed, it is a frequency modu-
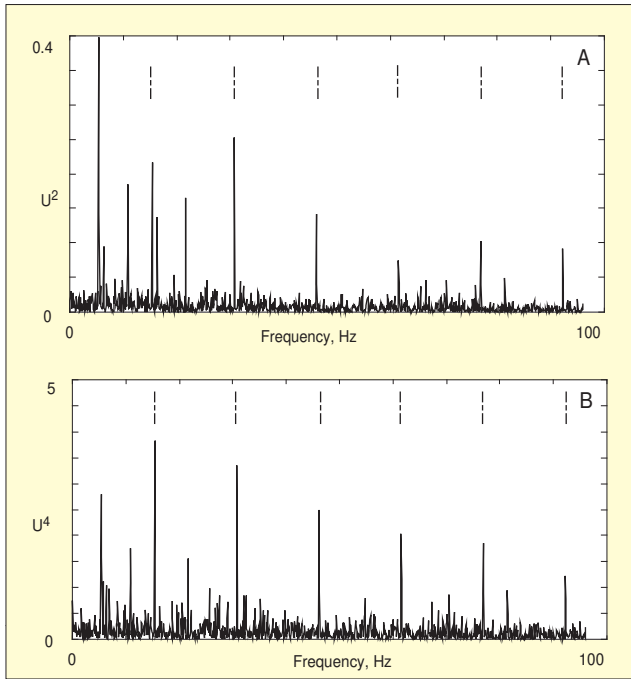
Figure 18. Advantage of analyzing the squared envelope (B) compared with the envelope (A). Note the enhancement of the harmonic series at 15.5 Hz (BPFO).

Figure 19. Procedure for envelope analysis using Hilbert Transform technique.

lation. There is no modulation term for the angular acceleration obtained by further differentiation. A mechanical example of amplitude modulation is the variation in vibration amplitude at the meshing frequency in a gearbox. The increase in tooth deflection with load gives an increasing departure from ideal involute profiles, and often tooth load varies periodically with the rotation of the gears.

Thus, a generally modulated signal can be represented by:

$$A_m(t)\cos\big(2\pi f_c t + \phi_m(t)\big) \qquad (16)$$

where $A_m(t)$ represents the amplitude modulation function and $\phi_m(t)$ represents the phase modulation function in radians. The corresponding frequency modulating function (in Hz) is

$$\frac{1}{2\pi}\frac{d\phi_m(t)}{dt}$$

Equation 16 is the real part of the rotating vector:

$$A_m(t)\ \exp\big\{j\big(2\pi f_c t + \phi_m(t)\big)\big\} \qquad (17)$$

whose modulus is the amplitude modulating function and whose phase is the phase modulating function plus the linear carrier component. Thus, if it is desired to demodulate a real signal such as Equation 16, it is desirable to find the corresponding imaginary part so as to form the complex Equation 17. Provided the fluctuating part of Equation 17,

$$A_m(t)\exp\big\{j\phi_m(t)\big\} \qquad (18)$$

has a half bandwidth less than the carrier frequency f_c, the spectrum of Equation 17 will be one-sided, and Equation 17 will be an analytic function. In this case the required imaginary part is the Hilbert transform of the real part. As the spectra of the two parts are convolved, the total bandwidth is less than the sum of the individual bandwidths. The bandwidth of the amplitude part is directly that of $A_m(t)$. Though $\exp(j\phi_m(t))$ is theoretically infinite, if the maximum phase deviation is less than 1 radian, the effective bandwidth (within the dynamic range) is less than twice that of $\phi_m(t)$.

Note that a zoom processor (Figure 8) can be used directly both to extract that part of the spectrum to be demodulated and to remove the carrier component by zooming at the carrier frequency. Generally, the zoom process results in a considerable reduction in the sampling rate to be more compatible with the bandw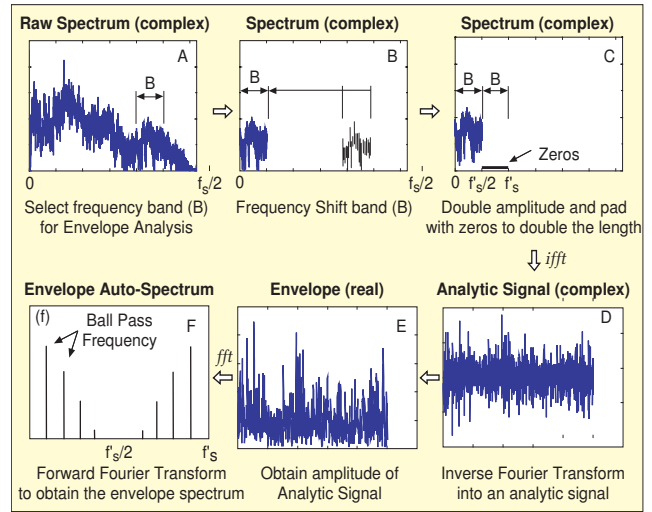idth of the modulating functions. The modulus of the complex output from the zoom processor is the amplitude modulating function, while the argument is the phase modulating function. This may have to be unwrapped to a continuous phase function (i.e., eliminating jumps over 2π), but in general this is not a problem for well-behaved functions. Demodulating a larger bandwidth decreases the time step, and thus phase jump, between samples and may facilitate unwrapping.

As illustrated in Figure 17, the same thing can be achieved using FFT transforms, although the first one will have to be large to accommodate the high carrier frequency while being long enough to contain sufficient periods of the lower modulating frequencies. Where phase demodulation is required, the center of the demodulation band will have to be shifted to zero frequency (and negative frequency components shifted to the other end of the frequency record). However, for amplitude demodulation the result is unaffected by the frequency shift. Further, it is more convenient to shift the left hand end of the band to zero frequency and pad the negative frequency side with zeros thus maintaining an analytic signal. In either case there should be at least as many contiguous zeros in the spectrum as components since the modulus is the square root of the amplitude squared and the latter corresponds to the convolution of the spectrum with its complex conjugate reversed end-for-end. The zeros prevent extraneous wrap-around errors.

Envelope Analysis. Figure 6 shows that for diagnostics of bearing signals, it is advantageous to frequency analyze the envelope of the bearing signal because of the smearing of the raw spectrum. The envelope signal has traditionally been obtained by rectification and lowpass filtration, but demodulation of the analytic signal (of Figure 17a) has an advantage – the bandpass filters used to extract the demodulation band are much sharper than typical analog bandpass filters and can better isolate the bearing signal from large adjacent masking components. Moreover, it is generally better to analyze the squared envelope rather than the envelope, as this improves the signal to noise ratio of the result.[8]

Figure 18 shows a typical example from a paper mill bearing with an outer race fault. The shaft speed is less than 2 Hz, and BPFO only 15.4 Hz. But, the demodulated band was in the range of 5.2-5.6 kHz where the largest spectral change occurred. The spectrum of the squared envelope in Figure 18b is much clearer than the normal envelope spectrum in Figure 18a.

Figure 19 shows the procedure for obtaining the envelope (or envelope squared) spectrum for a typical bearing fault. The band B is typically placed where the largest (dB) spectral change has occurred as a result of the bearing fault, since this is where the signal to noise ratio is the highest. After shifting this band to zero frequency and padding with zeros, the new sampling frequency is just 2B. B should thus be chosen to con-
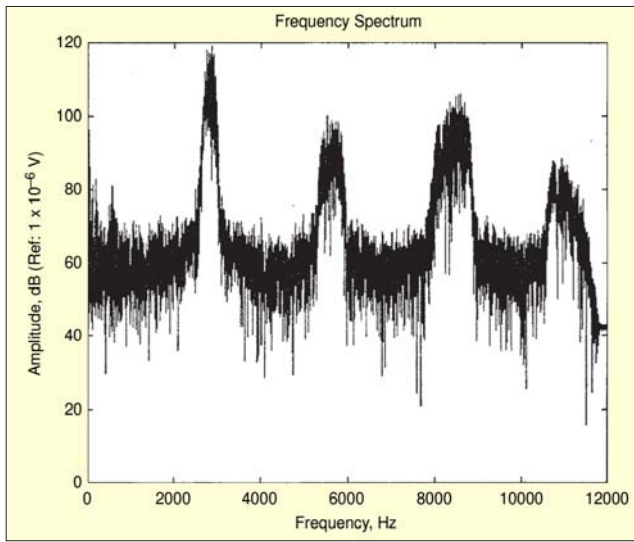
Figure 20. Spectrum of ring gear tooth passage signal showing four harmonics and their sidebands.

Figure 21. Unwrapped phase from demodulating the first harmonic of Figure 20.

tain a sufficiently wide range of frequency for diagnostic purposes, typically 4-5 harmonics of the highest fault frequency (usually BPFI). If the analytic signal represented by the one-sided spectrum of Figure 19c is denoted by $f(t)$, its squared envelope can be obtained as $f(t) \cdot f^*(t)$, meaning that the corresponding spectrum is given by $F(f) * F^*(-f)$, where $F(f)$ is the Fourier transform of $f(t)$. To obtain the envelope, it is necessary to take the square root, which introduces distortion.[8]

Phase and Frequency Demodulation. Phase and frequency demodulation is illustrated by the example of detecting misfire in an internal combustion (IC) engine by the pattern of angular velocity in the torsional vibration of a spark ignition engine. This is obtained by frequency demodulation of a shaft encoder signal, but the latter can be the pulses from a proximity probe detecting the passage of teeth on the ring gear.

Figure 20 shows the spectrum of such a signal. In principle, any harmonic of the tooth-pass frequency can be demodulated, as the speed variation gives rise to a fluctuation in the time intervals between pulses, which gives rise to a phase modulation proportional to the order of the harmonic demodulated, but otherwise of the same shape. To calibrate the result in terms of shaft angle, it is necessary to divide the measured phase signal by the shaft order demodulated. In this case the first toothpass harmonic was demodulated since it had the best signal to noise ratio.

Figure 21 shows the resulting phase signal where the slope means that the correct carrier frequency has not been chosen. If required, the slope can be removed by a 'detrend' operation.

To obtain the angular velocity it is necessary to differentiate the phase (angular displacement). This is best achieved by multiplying by $j\omega$ in the frequency domain since a bandpass filtration can be performed at the same time. Figure 22 shows the result of doing this with the phase signal of Figure 21.

In the angular velocity diagram of Figure 22, it is obvious that there is a misfire on cylinder 6 (actually caused by detaching the spark plug lead), as there is a rapid drop in speed where it should fire, which is gradually built up by the firing of the remaining cylinders. In a number of student projects, different faults were introduced and it became clear that a misfire could always be detected; although the reason for the misfire could not. Typical reasons for misfire that gave similar results were:
1. Failure of spark.
2. Faulty injection to one cylinder.
3. Simulated burnt valve by using an oversize pushrod. In this case the misfire was noticeably different because not only was the combustion pressure missing, but also the compression pressure.
4. A leaky valve simulated by using a loose spark plug. In this case there was a partial misfire that could in fact be quanti-
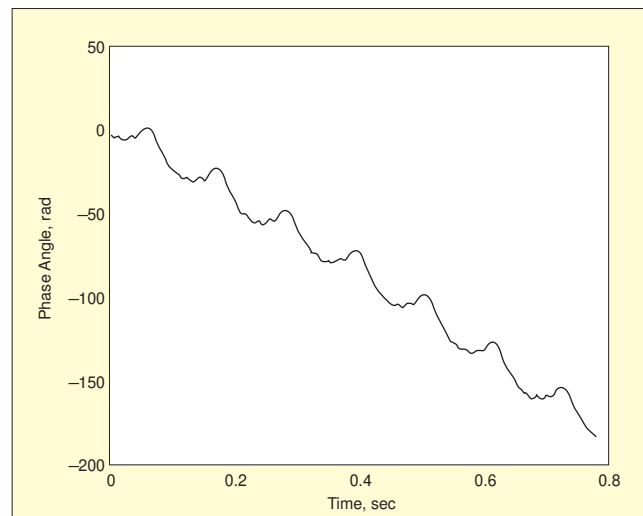
fied by the smaller jump in angular velocity for firing on cylinder 6 compared with the other cylinders.

The transmission error (TE) signal for a gear pair (as defined in gear faults section) can be obtained by demodulating the signals from a shaft encoder attached to each gear.[18] The TE signal can itself then be demodulated (with the toothmesh frequency as carrier) to highlight local faults. A similar demodulation carried out on acceleration signals was able to reveal a tooth root crack in a helicopter gearbox long before it became apparent using other techniques.[19]

Cyclostationary Signal Analysis

Next, the subject of cyclo-stationarity is examined in more detail, because of its relative novelty and its importance in separating different components in machine vibration signals.

Cyclostationary signals are defined as those whose second order statistics, such as their autocorrelation function, vary periodically. Strictly speaking, this defines second order cyclostationarity, as periodic signals can be considered as first order cyclostationary. Thus the bivariate autocorrelation function $R_x(t,\tau)$, defined by:

$$R_x(t,\tau) = E\left[x\left(t + \tfrac{\tau}{2}\right) x^*\left(t - \tfrac{\tau}{2}\right) \right] \qquad (19)$$

has the property that:

$$R_x(t,\tau) = R_x(t + T, \tau) \qquad (20)$$

where T is the periodic time.

Note that this definition is similar to that commonly used for stationary signals, except that (by definition) the statistics of the latter do not vary with time, and so it is expressed as a function of time shift τ only. Furthermore, it is common to displace only one of the signals by τ rather than make the displacement symmetrical about time t. However when the function varies with t it is better to use the symmetrical displacement to better assign the value to time t.

The autocorrelation function itself can be hard to interpret and so it is often further processed. A Fourier transform of the two-dimensional diagram in the t direction gives a result called the "instantaneous power spectrum," which is related to the Wigner-Ville distribution (WVD), a series of spectra varying with time.[20] The WVD is typically applied to a single time record and thus does not include the "expected value" or averaging operation in Equation 19. For cyclostationary signals, the instantaneous spectra vary periodically with time, so it is beneficial to perform a further Fourier transform (actually a Fourier series) with respect to time t in order to quantify this periodicity. The result is known as the "spectral correlation," and is used in some results given below. The formula is thus:

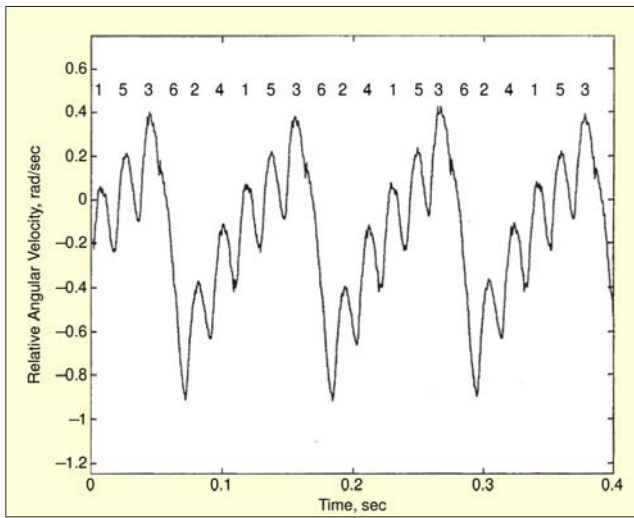$$S_x(\alpha, f) = \underset{t \to \alpha}{\Im}\ \underset{\tau \to f}{\Im}\ (R_x(t,\tau)) \qquad (21)$$

Figure 22. Angular velocity signal obtained as the derivative of the phase of Figure 21 (numbers along top denote cylinder firing cycle).

where f represents normal frequency, and α represents so-called "cyclic frequency."

The integral of the spectral correlation over all f in fact gives the same result as the Fourier analysis of the expected value of the squared signal, and so is very closely related to envelope analysis.[21] If $x(t)$ is an analytic signal,[8] the result is the spectrum of the "squared envelope," which as shown above gives better results for bearing diagnostics than the simple envelope obtained by amplitude demodulation.

Machine signals that repeat cyclically but are not directly phase-locked to shaft speeds are often cyclostationary. An example already mentioned is the signals associated with combustion in an IC engine. These can be decomposed into a periodic component (the expected value) and a second order cyclostationary component that is like amplitude modulated noise, so that its squared envelope is periodic. Rolling element bearing signals were modelled as cyclostationary[21] because of the random slip associated with the approximate periodicity. The signals are only approximately cyclostationary (termed pseudo-cyclostationary), but can usefully be treated as cyclostationary as a first approximation.[6] This is because the ballpass frequencies are not well defined because of the slip, as opposed to engine signals, which are constrained to the engine cycle frequency.

Figure 23[21] shows the spectral correlation for an inner race fault in a ball bearing, demonstrating that the harmonics of BPFI and sidebands spaced at shaft speed are distributed with f but discrete with respect to α. The integral of this over all f gives the same result as the spectrum of the squared envelope.

From this it would appear that the spectral correlation does not give any benefit over (squared) envelope analysis, but there is one situation where it does, illustrated in Figure 24. This is the case of an inner race fault in a helicopter gearbox that was detected so late that the spalling had extended about 1/3 of the way around the race and had become smoothed. This meant that high frequency pulses at BPFI were no longer generated, but envelope analysis revealed strong modulation at shaft speed. This is presumedly due to the varying support of the gear as the fault passed through the load zone, but how to distinguish this from a gear fault? The answer lies in the fact that a gear fault would give a deterministic modulation of the gear mesh signal, which gives discrete points in the spectral correlation in both the f and α directions. The rough inner race fault, on the other hand, gives a second order cyclostationary modulation since the rollers are in a different position on the spalled surface for each revolution of the gear. The effect in the spectral correlation is distributed with f, just as in Figure 23. The second order cyclostationary part would be combined with a first order part (the mean value of the modulating signal) but the effects from this can be removed, along with gear effects,
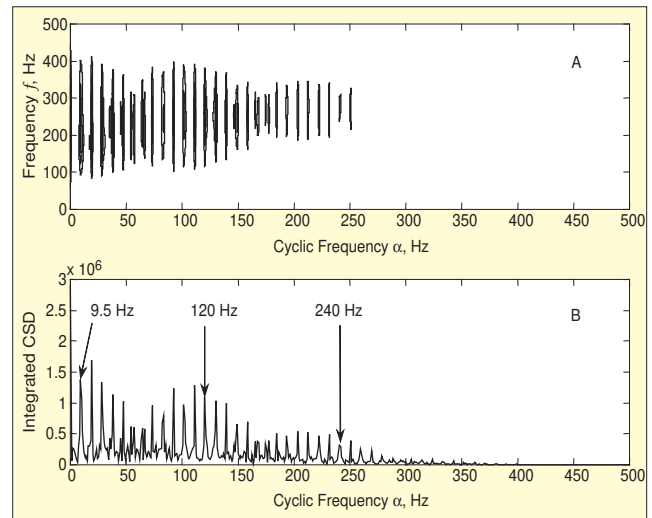

Figure 23. A – spectral correlation for a localized inner race fault (actual span of frequency f [2800; 3300] Hz), B – spectrum of squared evelope. Shaft speed = 9.5 Hz, BPFI = 120 Hz.
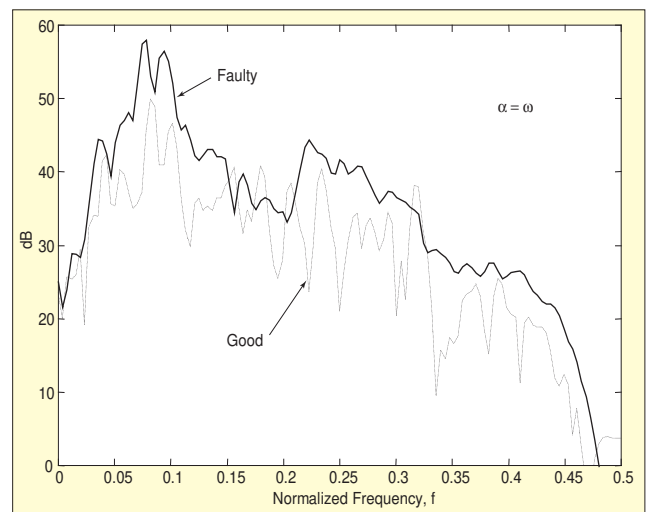

Figure 24. Spectral correlation for an extended inner race fault evaluated at $\alpha = \omega$.

by using discrete/random separation before calculating the spectral correlation. The latter can be evaluated for a specified value of cyclic frequency where a result is expected, such as the shaft speed Ω for an inner race fault. This eliminates stationary random noise, which only appears at zero cyclic frequency (it is constant with time). Thus, the only explanation for the considerable increase as a result of the fault in Figure 24 is a cyclostationary signal with cyclic frequency equal to the shaft speed, in other words a bearing inner race fault.

Prognosis

This is the least developed area in machine condition monitoring, but probably the one currently receiving the most attention.

For faults that develop gradually, it can be sufficient to simply carry out trend analysis of parameters that characterize the fault severity, such as the amount of change from a baseline value (e.g., exceedance spectra as in Figure 1). One system was proposed with this as its basis.[22] Note that since equal changes in severity are given by equal changes on a logarithmic scale, the trend plots should be of logarithmic values (e.g., dBs) as a linear trend of dB values represents a uniform change. Sometimes the fault severity feeds back on the rate of deterioration (e.g., with gear wear) in which case it may be better to fit an exponential curve to the data to make the best estimates of remaining life.

The best estimates of remaining life will be obtained from

models of the failure mechanism and much effort is currently being put into developing such models. This is probably most advanced in the application to rotor dynamics and it is expected that such models will soon be able to differentiate between unbalance, misalignment and rotor cracks, as well as being able to make valid prognoses of future developments. Such simulation models will also be very valuable to train neural networks to recognize a wide range of faults, as in general it would not be economically viable to experience such failures in sufficient numbers.

Conclusion

A large number of techniques are now available to use vibration analysis to detect and diagnose incipient faults in operating machines. Current developments will help in automating both the diagnosis and prognosis of such faults.

References

1. John S. Mitchell, *Machinery Analysis and Monitoring*, Penn Well, 1981.
2   E. Downham and R. Woods, ASME paper, Toronto, September 8-10, 1971.
3. P. Bradshaw and R. B. Randall, "Early Fault Detection and Diagnosis on the Trans Alaska Pipeline," MSA Session, ASME Conf., Dearborn, pp 7-17, 1983.
4. J. Howard Maxwell, "Induction Motor Magnetic Vibration," Proc. Vibration Institute, Meeting, Houston, TX, April 19-21, 1983.
5. R. B. Randall, "A New Method of Modeling Gear Faults," *ASME J. Mech. Design*, 104, pp 259-267, 1982.
6. J. Antoni and R. B. Randall, "Differential Diagnosis of Gear and Bearing Faults," *ASME J. Vib. & Acoustics*, 124, Apr 2002, pp. 165-171.
7. P. D. McFadden and J. D. Smith, "Model for the Vibration Produced by a Single Point Defect in a Rolling Element Bearing," *J. Sound Vib.*, 96 (1), pp 69-82, 1984.
8. D. Ho and R. B. Randall, "Optimisation of Bearing Diagnostic Techniques Using Simulated and Actual Bearing Fault Signals," *Mechanical Systems and Signal Processing*, 14 (5), September 2000, pp 763-788.
9. W. A. Gardner, *Introduction to Random Processes with Applications to Signals and Systems*, Macmillan, 1986.
10. R. B. Randall, "Frequency analysis," Brüel & Kjær, Copenhagen, 1987.
11. S. Braun and J. K. Hammond, "Parametric Methods," *Mechanical Signature Analysis*, (Ed. S. Braun), Academic Press, London, 1986.
12. Y. Gao, R. B. Randall and R. Ford, "Estimation of Envelope Spectra Using Maximum Entropy Spectral Analysis and Spectral Interpolation," *Int. J. of Comadem*, 1 (3), pp 15-22, 1998.
13. W. Wang and A. K. Wong, "Autoregressive Model-Based Gear Fault Diagnosis," *ASME J. Vib. & Acoustics*, 124, Apr. 2002, pp 172-179.
14. P. D. McFadden, "A Revised Model for the Extraction of Periodic Waveforms by Time Domain Averaging," *Mech. Systems & Signal Processing*, 1 (1), pp 83-95, 1987.
15. R. Potter and M. Gribler, "Computed Order Tracking Obsoletes Older Methods," SAE Paper 891131, 1989.
16. Chaturvedi, G. K. and Thomas, D. W., "Bearing Fault Detection Using Adaptive Noise Cancelling," Transactions of the ASME, 104, Apr. 1982, pp 280-289.
17. J. Antoni and R. B. Randall, "Unsupervised Noise Cancellation for Vibration Signals – Part II, A Novel Frequency Domain Algorithm." *Mechanical Systems and Signal Processing*, Vol. 18, No. 1, pp 103-118, 2004.
18. P. J. Sweeney and R. B. Randall, "Gear Transmission Error Measurement using Phase Demodulation," Proc. I. Mech. E., Part C, *J. Mech. Eng. Sci.* 210 (C3), pp 201-213, 1996.
19. P. D. McFadden. *J. Vib., Acoust., Str., & Rel. in Des.*, 108, pp 165-170.
20. L. Cohen, *Time-Frequency Analysis*, Prentice-Hall, NJ. 1995.
21. R. B. Randall, J. Antoni and S. Chobsaard, "The Relationship Between Spectral Correlation and Envelope Analysis in the Diagnostics of Bearing Faults and Other Cyclostationary Machine Signals," *Mech. Systems & Signal Processing*, 15(5), pp 945-962, 2001.
22. R. B. Randall, "Computer Aided Vibration Spectrum Trend Analysis for Condition Monitoring," *Maintenance Management International*, 5, 1985, pp 161-167.

The author can be contacted at: b.randall@unsw.edu.au.